Katrin Philipp, Angelos Filippatos, Nektarios Koukourakis, Robert Kuschmierz, Christoph Leithold, Albert Langkamp, Andreas Fischer, Jürgen Czarske

In-process deformation measurements of translucent high speed fibre-reinforced disc rotors

Erstveröffentlichung in / First published in:

International Conference on Optical and Photonic Engineering (icOPEN2015). Singapore, 2015. Bellingham: SPIE, Vol. 9524 *[Zugriff am: 02.05.2019]*.

DOI: https://doi.org/10.1117/12.2185090

In-process deformation measurements of translucent high speed fibre-reinforced disc rotors

Katrin Philipp, Angelos Filippatos, Nektarios Koukourakis, Robert Kuschmierz, Christoph Leithold, et al.

Katrin Philipp, Angelos Filippatos, Nektarios Koukourakis, Robert Kuschmierz, Christoph Leithold, Albert Langkamp, Andreas Fischer, Jürgen Czarske, "In-process deformation measurements of translucent high speed fibre-reinforced disc rotors," Proc. SPIE 9524, International Conference on Optical and Photonic Engineering (icOPEN 2015), 952407 (17 July 2015); doi: 10.1117/12.2185090

Event: International Conference on Optical and Photonic Engineering (icOPEN2015), 2015, Singapore, Singapore

In-process deformation measurements of translucent high speed fibre-reinforced disc rotors

Katrin Philipp[a], Angelos Filippatos[b], Nektarios Koukourakis[a], Robert Kuschmierz[a], Christoph Leithold[a], Albert Langkamp[b], Andreas Fischer[a] and Jürgen Czarske[a,*]

[a]Laboratory for Measurement and Sensor System Technology, TU Dresden, Germany;
[b]Institute of Lightweight Engineering and Polymer Technology, TU Dresden, Germany

ABSTRACT

The high stiffness to weight ratio of glass fibre-reinforced polymers (GFRP) makes them an attractive material for rotors e.g. in the aerospace industry. We report on recent developments towards non-contact, in-situ deformation measurements with temporal resolution up to 200 µs and micron measurement uncertainty. We determine the starting point of damage evolution inside the rotor material through radial expansion measurements. This leads to a better understanding of dynamic material behaviour regarding damage evolution and the prediction of damage initiation and propagation. The measurements are conducted using a novel multi-sensor system consisting of four laser Doppler distance (LDD) sensors. The LDD sensor, a two-wavelength Mach-Zehnder interferometer was already successfully applied for dynamic deformation measurements at metallic rotors. While translucency of the GFRP rotor material limits the applicability of most optical measurement techniques due to speckles from both surface and volume of the rotor, the LDD profits from speckles and is not disturbed by backscattered laser light from the rotor volume. The LDD sensor evaluates only signals from the rotor surface. The anisotropic glass fibre-reinforcement results in a rotationally asymmetric dynamic deformation. A novel signal processing algorithm is applied for the combination of the single sensor signals to obtain the shape of the investigated rotors. In conclusion, the applied multi-sensor system allows high temporal resolution dynamic deformation measurements. First investigations regarding damage evolution inside GFRP are presented as an important step towards a fundamental understanding of the material behaviour and the prediction of damage initiation and propagation.

Keywords: multi-sensor system, interferometry, signal processing, optics on surfaces

1. INTRODUCTION

The in-situ characterization of the material behavior of glass fibre-reinforced polymer (GFRP) disc rotors under dynamic load is an important step towards the development of novel, lightweight materials for several applications, e.g. the aerospace industry.[1] Monitoring the dynamic rotor deformation due to the centrifugal forces reveals information about damage initiation and development within the rotor volume.[2] This eventually leads to improved models of the material behavior and might allow predicting final rotor failure. However, typical rotor diameters of about 50 cm and radial expansions in the range of only a few 100 µm complicate the measurement of the dynamic rotor deformation. The application of strain gauges enables local deformation measurements.[3] However, they can rip of due to the high rotational speeds, if they are attached on the rotor surface. Integrated strain gauges are invasive and may change the rotor behaviour under dynamic load. Electrical sensors like capacitive, inductive or eddy current probes are well-established for measurements at metallic rotors, but the low magnetic permeability and electrical conductivity restricts the applicability at composite rotors.[4] Placing several optical distance sensors around the circumference of the rotor enables the contact-less, destruction-free measurement of the radial expansion.[5] In contrast to optical sensors like triangulation,[6] chromatic confocal sensing[7] and optical coherence tomography,[8] laser Doppler distance sensors are suitable for measurements at high surface velocities.[2] However, the precision of previous measurements of the radial expansion using three laser Doppler distance sensors is limited to about 30 µm at temporal resolutions of one rotor revolution.[2] Since the laser Doppler distance sensor has been optimized for the application at the investigated rotor material, the measurement precision is

---

*Corresponding author: juergen.czarske@tu-dresden.de

International Conference on Optical and Photonic Engineering (icOPEN 2015), edited by Anand K. Asundi, Yu Fu,
Proc. of SPIE Vol. 9524, 952407 · © 2015 SPIE · CCC code: 0277-786X/15/$18 · doi: 10.1117/12.2185090

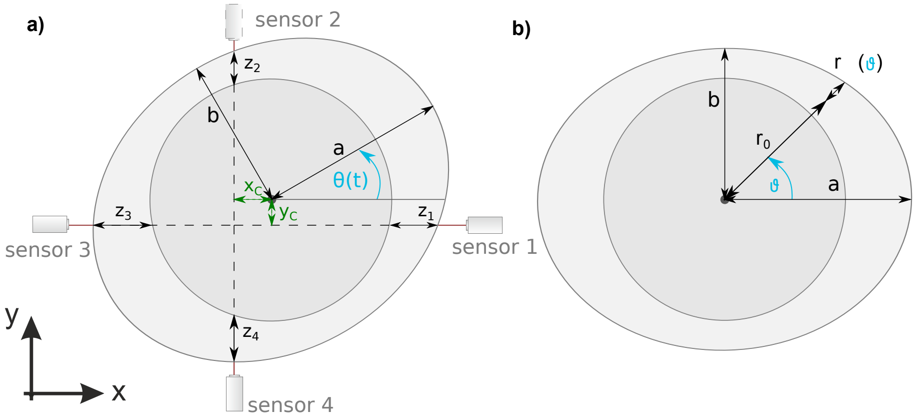

Figure 1: Left: Setup of multi-sensor system consisting of four sensors equally distributed along the circumference of the rotor. Right: Illustration of the radial expansion $r_\Delta(\vartheta)$ with major and minor axis a and b of ellipse, respectively.

mainly limited by the signal processing. In particular, tumbling motions with amplitudes up to 150 µm at the used test rig[5] were not taken into account in previous measurements[2] and are the main restriction of achieved measurement precision. The aim of this contribution is the reduction of achievable measurement uncertainties by taking into account the tumbling motion of the rotor. Additionally the applicability of the laser Doppler sensor at translucent materials is demonstrated.

2. MULTI-SENSOR SYSTEM

2.1 Multi-sensor system

The multi-sensor system consists of four distance sensors equally distributed along the circumference of the rotor (Fig. 1a). The sensor shape is defined by the rotor radius $r = r_0 + r_\Delta$, that consists of the initial radius r_0 of the rotor at rest and the radius expansion r_Δ (Fig. 1b). Note that the time dependency of the variables is not explicitly denoted for better readability. The tumbling motion is described by the rotor center position (x_c, y_c) and the current rotor orientation by $\theta = \omega t$. The corresponding rotational frequency ω is obtained by an inductive rotational speed sensor. The sensor signals $z_i, i = 1, 2, 3, 4$ specify the distance between the rotor surface position at the beginning of the measurement and current rotor surface. Thus, the sensor signals contain a superposition of radial expansion and tumbling motion of the rotor. The simultaneous determination of radial expansion and rotor center position is the measurement task to be solved by the signal processing algorithm.

2.2 Signal processing

The aim of the signal processing algorithm is the simultaneous determination of the radial rotor expansion $r_\Delta(\vartheta, t)$ and the rotor center position (x_c, y_c). At a given time, the four sensors deliver the sensor distance signals $z_i(t), i = 1, 2, 3, 4$. The current rotor orientation $\theta = \omega t$ is determined using an inductive rotational speed sensor. The assuming of small tumbling motion amplitudes yields the simplified equation system

$$z_i = r_\Delta(\phi_i - \theta) + x_c \cos(\phi_i) + y_c \sin(\phi_i), \tag{1}$$

with the angular sensor positions $\phi_i = (i-1) \cdot \pi/2$. The equation system resulting from Eq. (1) at a given measurement time t is underdetermined, since it consists of four equations and 12 parameters. Thus, additional assumptions have to be made.

The state-of-the-art approach[2] assumes converging tumbling motion and applies temporal averaging to Eq. (1) over integer multiples of the rotor revolution time $T_{\text{revolution}} = 2\pi/\omega$. In order to combine the information of all sensors at a given rotor angle ϑ, the sensor signals are time-shifted

$$\tilde{z}_i(t) = z_i(t + \phi_i/2\pi \cdot T_{\text{revolution}}). \tag{2}$$

The radial expansion is then determined by averaging over all four sensor signals and over all measured points, i.e.

$$r_\Delta(\vartheta) = \frac{1}{4N_r} \sum_{i=1}^{4} \sum_{n_r=0}^{N_r-1} \tilde{z}_i(n_r \cdot T_{\text{revolution}}) \tag{3}$$

Consequently, the state-of-the-art approach enables the determination of arbitrary (convex) rotor expansions at the cost of temporal and expansion resolution. If the tumbling motion does not converge as at the used test rig,[5] the measured rotor expansion is distorted, leading to increased measurement uncertainties of the determined radius expansion.

In order to take the tumbling motion into account, the equation system (1) is solved analytically. This yield the solution

$$a(t) = \frac{A(t)}{2} \sqrt{\cos^2(\theta(t)) + \sin^2(\theta(t)) \frac{A^2(t)\cos^2(\theta(t)) - B^2(t)\sin^2(\theta(t))}{B^2(t)\cos^2(\theta(t)) - A^2(t)\sin^2(\theta(t))}} \tag{4}$$

$$b(t) = \frac{B(t)}{2} \sqrt{\cos^2(\theta(t)) + \sin^2(\theta(t)) \frac{B^2(t)\cos^2(\theta(t)) - A^2(t)\sin^2(\theta(t))}{A^2(t)\cos^2(\theta(t)) - B^2(t)\sin^2(\theta(t))}} \tag{5}$$

$$x_c(t) = \frac{1}{2}\left[z_1(t) - z_3(t)\right] \tag{6}$$

$$y_c(t) = \frac{1}{2}\left[z_2(t) - z_4(t)\right] \tag{7}$$

with $B(t) = 2r_0 + z_2(t) + z_4(t)$ and $A(t) = 2r_0 + z_1(t) + z_3(t)$. As a result, the analytic signal processing algorithm enables the full reconstruction of the elliptic rotor shape as well as the tumbling motion at each single measurement time.

3. MEASUREMENTS AT TRANSLUCENT MATERIALS

Backscattered laser light from the surface as well as the rotor volume makes the applicability of optical measurement techniques challenging. It is shown, that the laser Doppler distance sensor (LDDS) provides robust and reliable distance measurements and consequently can be applied for dynamic deformation measurements at translucent materials.

3.1 Laser Doppler distance sensor

The laser doppler distance sensor (LDDS) is a two-wavelength Mach-Zehnder interferometer, that is based on the well-established laser Doppler velocimetry (Fig. 2). The distance z is determined by generating a converging and diverging interference fringe system, respectively. The distance z is then obtained by

$$z = q^{-1}\left(\frac{f_{\text{D}-}}{f_{\text{D}+}}\right), \quad v \approx \frac{1}{2}\left[f_{\text{D}+}d_+(z) + f_{\text{D}-}d_-(z)\right] \tag{8}$$

with the inverted calibration function q^{-1}, the fringe spacing functions $d_\pm(z)$ and the measured Doppler frequencies $f_{\text{D}\pm}$. The unambiguous calibration function

$$q(z) = \frac{d_+(z)}{d_-(z)} = \frac{f_{\text{D}-}}{f_{\text{D}+}} \tag{9}$$

is previously determined by calibration. Note that the LDDS also measures the lateral velocity v, but is not required for the multi-sensor system proposed here.

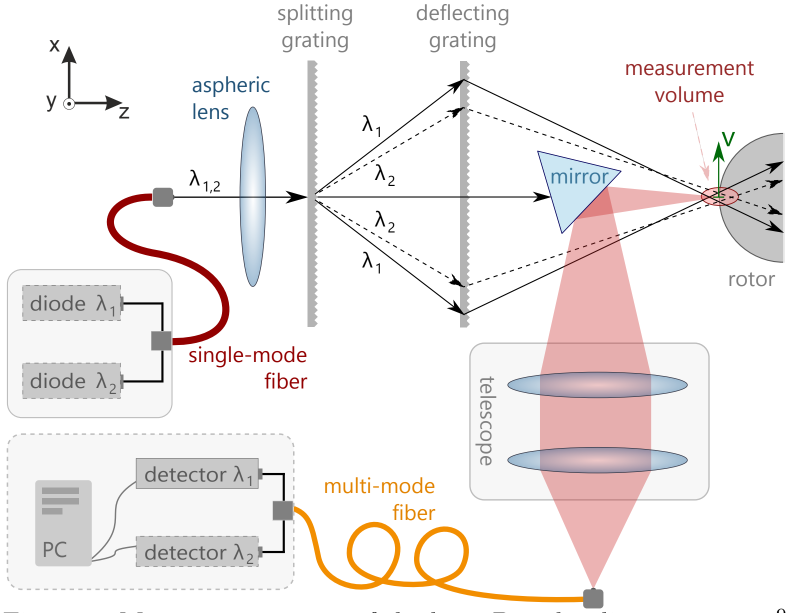

Figure 2: Measurement setup of the laser Doppler distance sensor.[9]

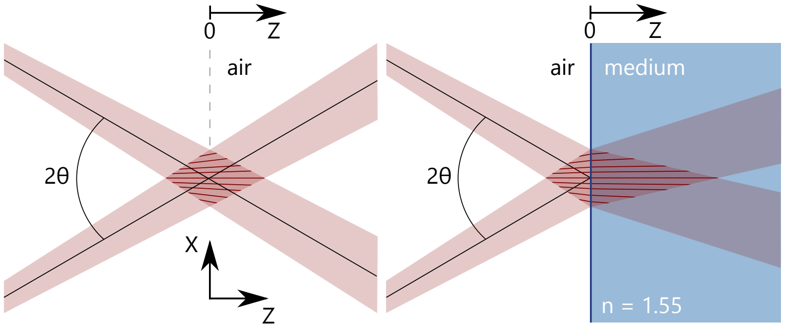

Figure 3: Scheme (not to scale) of undisturbed diverging interference fringe system (left) and deformation due to refraction at the material (right).[9]

3.1.1 Influence of translucence on measurement

In contrast to metallic surfaces, the main part of incoming light propagates into the volume of translucent materials and might be backscattered. It has to be ensured, that the backscattered light does not disturb the measurement. In order to investigate the influence on the measurement principle, refraction and dispersion of the laser beam at the surface is taken into account for the calculation of the changed measurement volume (Fig. 3). The slope of the fringe spacing curves $q_\pm$ decreases, leading to a decreased slope of the calibration function $q(z)$ (Fig. 4). As a consequence, backscattered light from the material volume causes shifted Doppler frequencies in comparison to light scattered at the surface. However, the roughness of the surface has not been taken into account for these considerations. Simulations with varying surface properties show, that the interference fringe system is destroyed above a certain roughness threshold (Fig. 5). Since the roughness of the investigated rotor is above the threshold, backscattered light from the rotor volume does not lead to disturbed measurement of the LDDS. Consequently, the LDDS is a sufficient tool for the multi-sensor system applied at translucent rotors.

4. VALIDATION OF THE MULTI-SENSOR SYSTEM

In order to validate the multi-sensor system, radial expansion measurements are conducted at glass-fibre-reinforced polymer rotors with rotational speeds between 600 rpm and 7200 rpm. The dynamic rotor deformation is expected to be elliptical due to the anisotropic orientation of the glass fibre reinforcement, as listed in Table 1. In order to validate the applicability of the novel signal processing algorithm, the elliptical shape of the expanded

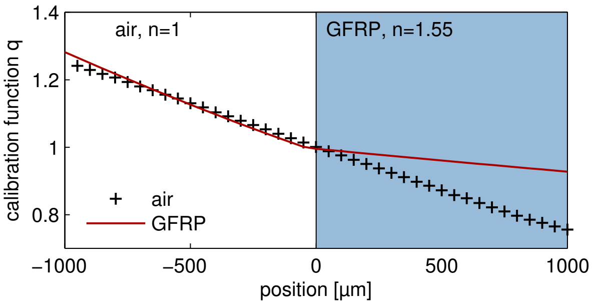

Figure 4: Measured calibration function $q_{\pm}(z)$ in air and calculated calibration function with medium placed at $z = 0$.

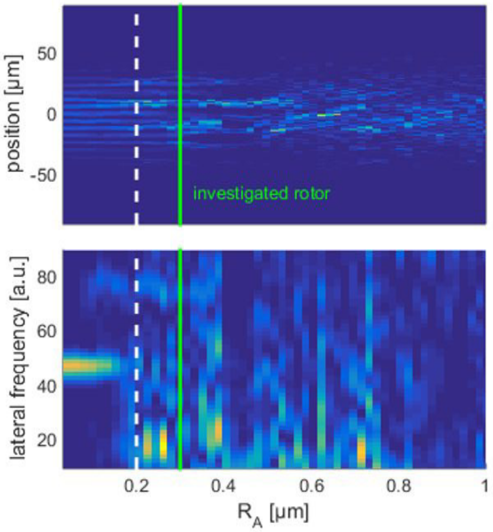

Figure 5: Lineprofiles simulated at $z = 20\,\mu\text{m}$ for increasing surface roughness (top) and corresponding Fourier transform (bottom) for investigated GFRP rotor (right). The roughness R_{A} of the investigated rotor is marked green and the corresponding threshold is indicated by the white dashed line.

rotor has to be confirmed. Consequently, the angular resolved radial rotor expansion is obtained by the temporal averaging algorithm and compared to elliptic fit functions. As depicted in Fig. 6a as an example for a rotor in the 3^{rd} damage state at rotational speeds of 600 rpm and 6000 rpm, the measured data is in good agreement to the fit functions. Since the residuals are distributed stochastically around the fits (Fig. 6b), the rotor faces elliptical expansion and the application of the extended signal processing algorithm is justified.

The analytic approach enables the isolation of the tumbling motion of the rotor (Fig. 7). In order to characterize the precision of the measurement system in dependency of the tumbling amplitude, the tumbling amplitude is determined using the analytic algorithm due to its high sampling frequency of 3 kHz. As illustrated in Fig. 7 for a rotational speed of 1800 rpm, the tumbling motion can be extracted from the sensor signals. In order to determine the mean tumbling amplitude for a given rotational speed, the tumbling radius

$$r_c(t_n) = \sqrt{(x_c(t_n))^2 + (y_c(t_n))^2} \tag{10}$$

is introduced as the geometric distance between current rotor centre position and origin of sensor-fixed coordinate system. The tumbling amplitude

$$A_{\text{T}} = \frac{1}{N}\sum_{n=1}^{N} r(t_n) \tag{11}$$

Table 1: Layout of the multi-ply multi-axial fabric used as reinforcement for the investigated rotor.

	orientation	filament type	mass percentage
reinforcement	0 °	GF-Roving 2400 tex and 1200 tex	48.7 %
reinforcement	−45 °	GF-Roving 300 tex	23 %
reinforcement	90 °	GF-Roving 200 tex	4.8 %
reinforcement	45 °	GF-Roving 300 tex	23 %
stitch		PES filament yarn 5 tex tricot300 tex	0.5 %

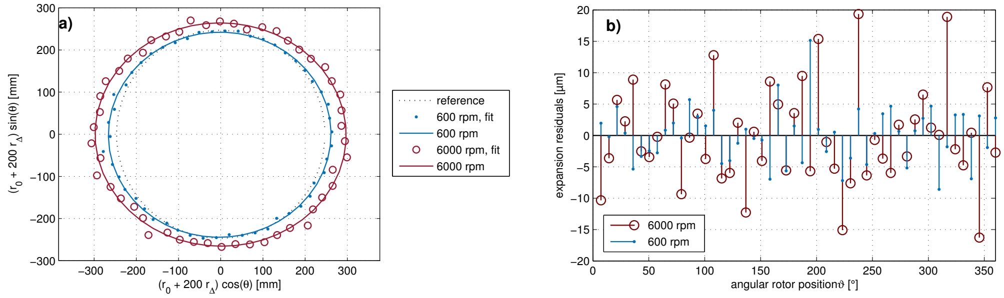

Figure 6: Dynamic expansion of investigated rotor at rotational speeds of 600 rpm and 6000 rpm obtained by applying temporal averaging. Note that the rotor expansion is magnified by a factor of 200 for better visibility. Since the residuals are distributed stochastically around the fits, the rotor faces elliptical expansion and, thus, applying the improved fitting algorithm is justified.

is then obtained by averaging over all measurements $n = 1, 2, \ldots, N$. At a rotational speed of 1800 rpm, the tumbling frequency both in x- and y-direction equals 3.1 Hz, i.e. 10.4 % of the rotational frequency. The tumbling amplitude is $A_\mathrm{T} = 120.5\ \mu\mathrm{m}$ at a rotational speed of 1800 rpm. Consequently the tumbling frequency and amplitude is in the same order of magnitude than previous measurements at metallic rotors with solely circular expansion.[5]

As depicted in Fig. 8, the measurement uncertainties of the rotor expansion for measurements conducted over a full rotor revolution in dependency of the tumbling amplitude A_T are in good agreement to simulations. The uncertainties by using the temporal averaging algorithm increase with the tumbling amplitude and are in the range from 30 µm to 60 µm. In contrast, the uncertainties obtained by using the analytic signal processing algorithm are independent of the tumbling amplitude and about 10 µm. Consequently the precision is improved

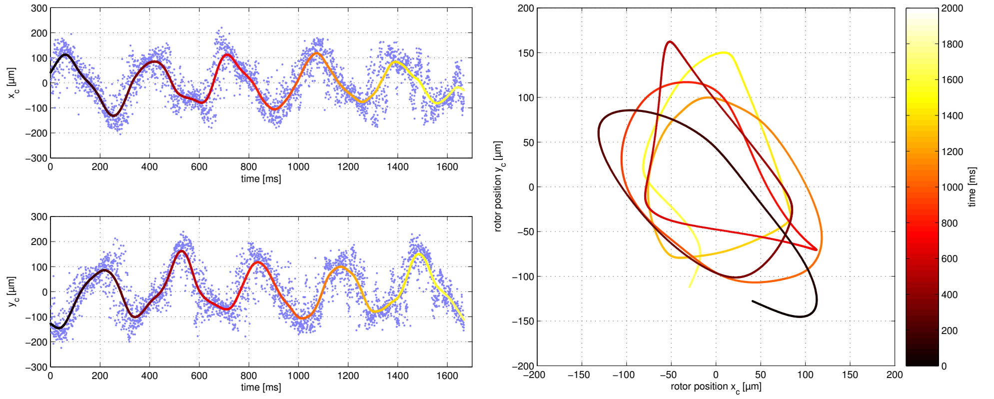

Figure 7: Tumbling motion of rotor at a rotational speed of 1800 rpm in x- and y-direction (left) and as an two dimensional map (right). The tumbling frequency both in x- and y-direction equals 3.1 Hz, i.e. 10.4 % of the rotational frequency and the tumbling amplitude is $A_\mathrm{T} = 120.5\ \mu\mathrm{m}$.

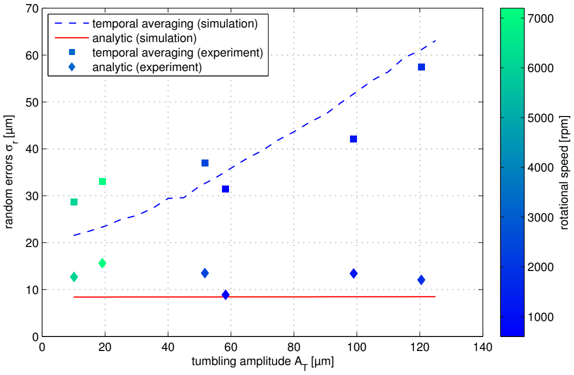

Figure 8: Measurement uncertainties σ_{r_Δ} for rotor expansion using the temporal averaging and analytic signal processing algorithms in dependency of tumbling amplitude A_T for measurement times of one full rotor revolution.

by a factor of three to six compared to the temporal averaging algorithm.

Averaging over N consecutive measured rotor revolutions yields the reduced mean 95 % confidence $t\sigma_{r_\Delta}/\sqrt{N}$ for the angle resolved rotor expansion with the factor t of the corresponding Student's t-distribution. Since measurements were conducted over $N \approx 40$ rotor revolutions with $t = 2.021$, a measurement uncertainty of 3 µm is achieved. In order to achieve a sub-micron measurement precision, an averaging over 65 rotor revolutions has to be applied.

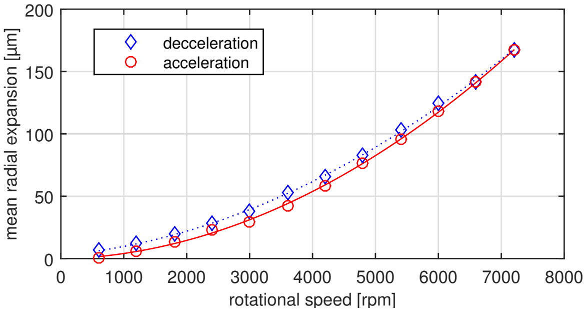

Figure 9: Mean radial rotor expansion with increasing and decreasing rotational speeds, respectively.

As a first demonstration of the applicability of the multi-sensor system, the mean radial expansion in dependency of the rotational speed is measured (Fig. 9). The acceleration as well as the deceleration curve are in good agreement to the quadratic fit with a deviation of 850 nm only.

5. CONCLUSION

The applicability of the multi-sensor system consisting of four equally distributed LDDS for dynamic radial expansion measurements at translucent glass fibre-reinforced polymer rotors was demonstrated. The effect of the translucent material on the measurement principle of the LDDS was investigated. Backscattered light from the rotor volume does not lead to systematic errors as was shown by simulations. Exploiting the knowledge of the elliptic rotor shape enables the simultaneous determination of the rotor expansion and the tumbling motion with measurement rates of 3 kHz. Micron measurement precision of the angular resolved rotor expansion is achieved at temporal revolutions corresponding to one rotor revolution. This correlates to an improvement of the expansion precision by a factor three to six compared to the state-of-the-art approach (depending on the tumbling amplitude). The mean expansion of the rotor is obtained with sub-micron precision for measurement times of

$40 \cdot T_{\mathrm{revolution}}$. In conclusion, the proposed multi-sensor system is an appropriate tool for the characterization of the dynamic expansion of fibre-reinforced composite rotors.

ACKNOWLEDGMENTS

The financial support from the Deutsche Forschungsgemeinschaft (funding code CZ 55/23-1 and HU 403/33-1) is gratefully acknowledged.

REFERENCES

1. C. Bakis, L. Bank, V. Brown, E. Cosenza, J. Davalos, J. Lesko, A. Machida, S. Rizkalla, and T. Triantafillou, "Fiber-Reinforced Polymer Composites for ConstructionState-of-the-Art Review," *Journal of Composites for Construction* **6**(2), pp. 73–87, 2002.
2. R. Kuschmierz, A. Filippatos, P. Günther, A. Langkamp, W. Hufenbach, J. Czarske, and A. Fischer, "In-process, non-destructive, dynamic testing of high-speed polymer composite rotors," *Mechanical Systems and Signal Processing* **54-55**, pp. 325–335, Mar. 2015.
3. F. Gasco, P. Feraboli, J. Braun, J. Smith, P. Stickler, and L. DeOto, "Wireless strain measurement for structural testing and health monitoring of carbon fiber composites," *Composites Part A: Applied Science and Manufacturing* **42**, pp. 1263–1274, Sept. 2011.
4. D. Subramani, V. Ramamurti, and K. Sridhara, "Numerical analysis and experimental verification of the radial growth of a turbocharger centrifugal compressor impeller," *The Journal of Strain Analysis for Engineering Design* **32**(2), pp. 119–128, 1997.
5. P. Günther, F. Dreier, T. Pfister, J. Czarske, T. Haupt, and W. Hufenbach, "Measurement of radial expansion and tumbling motion of a high-speed rotor using an optical sensor system," *Mechanical Systems and Signal Processing* **25**(1), pp. 319–330, 2011.
6. R. G. Dorsch, G. Häusler, and J. M. Herrmann, "Laser triangulation: fundamental uncertainty in distance measurement," *Applied Optics* **33**(7), pp. 1306–1314, 1994.
7. A. K. Ruprecht, K. Koerner, T. F. Wiesendanger, H. J. Tiziani, and W. Osten, "Chromatic confocal detection for high-speed microtopography measurements," 2004.
8. D. Markl, G. Hannesschläger, A. Buchsbaum, S. Sacher, J. G. Khinast, and M. Leitner, "In-line quality control of moving objects by means of spectral-domain OCT," *Optics and Lasers in Engineering* **59**, pp. 1–10, Aug. 2014.
9. K. Philipp, N. Koukourakis, R. Kuschmierz, C. Leithold, A. Fischer, and J. Czarske, "Optical dynamic deformation measurements at translucent materials," *Optics Letters* **40**(4), pp. 514–517, 2015.